# *The frontal aslant tract underlies speech fluency in persistent developmental stuttering*

**Vered Kronfeld-Duenias, Ofer Amir, Ruth Ezrati-Vinacour, Oren Civier & Michal Ben-Shachar**

**Brain Structure and Function**

ISSN 1863-2653
Volume 221
Number 1

Brain Struct Funct (2016) 221:365-381
DOI 10.1007/s00429-014-0912-8

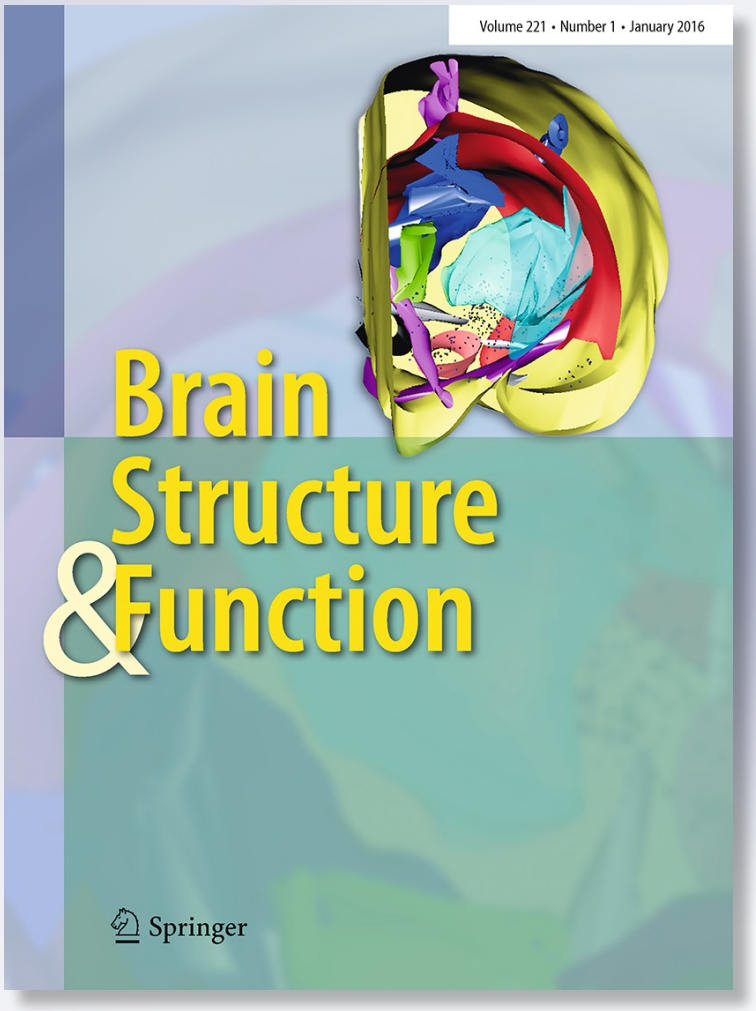


Springer

Brain Struct Funct (2016) 221:365–381
DOI 10.1007/s00429-014-0912-8

ORIGINAL ARTICLE

# The frontal aslant tract underlies speech fluency in persistent developmental stuttering

**Vered Kronfeld-Duenias · Ofer Amir · Ruth Ezrati-Vinacour · Oren Civier · Michal Ben-Shachar**

Received: 16 June 2014 / Accepted: 6 October 2014 / Published online: 26 October 2014


**Abstract** The frontal aslant tract (FAT) is a pathway that connects the inferior frontal gyrus with the supplementary motor area (SMA) and pre-SMA. The FAT was recently identified and introduced as part of a "motor stream" that plays an important role in speech production. In this study, we use diffusion imaging to examine the hypothesis that the FAT underlies speech fluency, by studying its properties in individuals with persistent developmental stuttering, a speech disorder that disrupts the production of fluent speech. We use tractography to quantify the volume and diffusion properties of the FAT in a group of adults who stutter (AWS) and fluent controls. Additionally, we use tractography to extract these measures from the corticospinal tract (CST), a well-known component of the motor system. We compute diffusion measures in multiple points along the tracts, and examine the correlation between these diffusion measures and behavioral measures of speech fluency. Our data show increased mean diffusivity in bilateral FAT of AWS compared with controls. In addition, the results show regions within the left FAT and the left CST where diffusivity values are increased in AWS compared with controls. Last, we report that in AWS, diffusivity values measured within sub-regions of the left FAT negatively correlate with speech fluency. Our findings are the first to relate the FAT with fluent speech production in stuttering, thus adding to the current knowledge of the functional role that this tract plays in speech production and to the literature of the etiology of persistent developmental stuttering.

**Keywords** White matter · Diffusion imaging · Fiber tracking · Fluency · Frontal aslant tract · Corticospinal tract

## Introduction

The frontal aslant tract (FAT) is a newly identified tract (Catani et al. 2012) that connects the inferior frontal gyrus (IFG) with supplementary and pre- supplementary motor areas (SMA and pre-SMA, respectively). Recently, FAT was introduced as part of a "motor stream" that plays an important role in speech production (Dick et al. 2013), complementing the accepted dorsal and ventral language streams (Hickok and Poeppel 2007). Several recent studies suggest that FAT plays a role in speech production. First, the volume of the FAT is left lateralized in right handed individuals (Catani et al. 2012), similar to other language-related pathways such as the long segment of the superior longitudinal fasciculus (Thiebaut de Schotten et al. 2011). Second, intraoperative electrical stimulation of the left FAT results in speech arrest (Vassal et al. 2014). In addition, in primary progressive aphasia, microstructural measures of the left FAT correlate with speech fluency

**Electronic supplementary material** The online version of this article (doi:10.1007/s00429-014-0912-8) contains supplementary material, which is available to authorized users.

V. Kronfeld-Duenias (✉) · O. Civier · M. Ben-Shachar
The Gonda Multidisciplinary Brain Research Center, Bar-Ilan University, 5290002 Ramat-Gan, Israel
e-mail: vered.kronfeld@gmail.com

M. Ben-Shachar
e-mail: michalb@mail.biu.ac.il

O. Amir · R. Ezrati-Vinacour
Department of Communication Disorders, Sackler Faculty of Medicine, Tel-Aviv University, Tel-Aviv, Israel

M. Ben-Shachar
Department of English Literature and Linguistics, Bar-Ilan University, 5290002 Ramat-Gan, Israel

measured using a story telling task (Catani et al. 2013). In this study, we specifically target the FAT and examine its contribution to persistent developmental stuttering, a speech disorder that affects a person's ability to fluently produce speech.

Persistent developmental stuttering is a speech disorder primarily characterized by prolongations, blocks and repetitions of sounds or syllables that occur while a person attempts to produce speech. These breakdowns in the production of fluent speech (stuttering events) are sometimes associated with other symptoms such as eye blinking, jaw jerking and other involuntary movements termed secondary or associated behaviors (Bloodstein and Ratner 2008). While this description of stuttering events clearly depends on motor aspects of speech production, it has previously been postulated that multiple factors interact in producing these disfluencies (Smith 1999; Smith et al. 2012). Specifically, one theoretical approach suggests that the motor difficulties observed during stuttering events are in fact the result of a core deficit in linguistic processing (Perkins et al. 1991; Postma and Kolk 1993). Persistent developmental stuttering therefore lies at the border between several systems including the motor and language networks, thus providing a unique opportunity to study the interface between these domains.

Producing fluent speech requires precise temporal coordination between distant brain regions. Indeed, functional imaging studies of persistent developmental stuttering, in which the fluent production is disturbed, indicate atypical patterns of activation in a wide network of cortical and sub-cortical regions including the right frontal operculum, bilateral auditory cortices, cerebellum and basal ganglia (for reviews, see Alm 2004; Brown et al. 2005). The distributed nature of these functional differences suggests that persistent developmental stuttering may be associated with atypical properties of white matter pathways, not only with specific localized cortical damage. Indeed, in the last decade, several studies have examined structural white matter differences between people who stutter and neurotypical controls.

The most replicable finding in studies of white matter in persistent developmental stuttering concerns fractional anisotropy (FA) reductions in the left Rolandic operculum (Chang et al. 2008; Connally et al. 2013; Cykowski et al. 2010; Sommer et al. 2002; Watkins et al. 2008), located caudally to Brodmann area 44 (BA44) and close to the primary motor representation of tongue, larynx and pharynx. Typically, differences in the left Rolandic operculum were ascribed to the superior longitudinal fasciculus/arcuate fasciculus (Chang et al. 2008; Connally et al. 2013; Cykowski et al. 2010; Watkins et al. 2008), a well-known pathway that is considered part of the language network (Hickok and Poeppel 2007). A second replicable finding is FA reduction in the corticospinal tracts (CSTs) of the motor network. Bilateral FA reductions in the CST were previously reported in children who stutter (Chang et al. 2008) as well as in adults who stutter (Cai et al. 2014). One study in adolescents and young individuals who stutter, reported that these FA differences are restricted to the right CST (Watkins et al. 2008), while another study showed a significant difference between the FA values measured in the left CST and those measured in the right CST of people who stutter compared with the same measurements calculated in controls (Connally et al. 2013). Differences in the left Rolandic operculum as well as in the CST suggest that both language pathways and motor connections are suspected contributors to persistent developmental stuttering.

To the best of our knowledge, ours is the first attempt to examine the role of the FAT in persistent developmental stuttering. However, the potential involvement of this tract in persistent developmental stuttering is implied by previous reports of structural and functional stuttering-related anomalies in the cortical endpoints of this tract: the IFG and the pre-SMA/SMA. Studies in people who stutter show gray matter volume differences in IFG (Beal et al. 2007, 2013; Cai et al. 2014; Chang et al. 2008; Kell et al. 2009) as well as white matter volume differences (Jäncke et al. 2004) and anisotropy reductions (Connally et al. 2013; Watkins et al. 2008) underneath this region. Comparing spontaneous recovery from persistent developmental stuttering with therapy-induced recovery, one study suggested the IFG as the only neural marker of optimal repair (Kell et al. 2009). Structural and functional differences related to persistent developmental stuttering were also reported in the SMA (Brown et al. 2005; Chang et al. 2008, 2011; Lu et al. 2010b). One recent study used graph theory and reported a lower degree of centrality in left SMA of adults who stutter (AWS) compared with fluent controls, indicating that the left SMA may serve as a hub in the speech network of the typical population but not in persistent developmental stuttering (Cai et al. 2014). The functionality of the IFG and SMA in typical populations, along with previous reports of their involvement in persistent developmental stuttering, suggests that the tract that connects these regions, the FAT, may play a role in this disorder.

In this study, we use diffusion magnetic resonance imaging and tractography to study the FAT in persistent developmental stuttering. We identify the FAT bilaterally in a group of AWS as well as in neurotypical adults. In addition, we identify the CST, a well-known motor tract which has previously been related to persistent developmental stuttering. We compare the volume estimations and average diffusion properties of these tracts in AWS vs. controls and complement this analysis with a more sensitive comparison of diffusion properties along the entire

**Table 1** Subject demographics and fluency measures

| | AWS (N = 15) | Controls (N = 19) | Significance level |
|---|---|---|---|
| Age (years) | 31.733 (9.93) | 33.26 (9.91) | n.s |
| Gender | 12M/3F | 16M/3F | n.s |
| Handedness[a] | 96 (8.28) | 89.63 (17.84) | n.s |
| Education[b] (years) | 14.7 (2.86) | 15.31 (2.8) | n.s |
| Speech rate (#SPS) | 4.7 (1.18) | 5.96 (0.78) | $p < 10^{-3}$ |
| SLD (%) | 12.36 (16.73) | 2.17 (1.03) | $p < 0.05$ |
| St. Syll. (%) | 7.86 (3.95) | 2.1 (0.99) | $p < 10^{-6}$ |

Mean values and standard deviations (in parentheses) are shown for the AWS and the control participants

*AWS* adults who stutter, *SPS* syllables per second, *SLD* stuttering-like-disfluencies, *St. Syll.* stuttered syllables, *n.s* not significant, *M* male, *F* female

[a] Handedness scores are based on the Edinburgh handedness inventory (Oldfield 1971). 100 indicate full right handedness, −100 indicate full left handedness

[b] Education data is missing in two AWS, therefore in this parameter, $N = 13$ in this group

extent of the tract. Last, we correlate the diffusivity measures extracted from the tract profiles with a behavioral measure of speech fluency. By studying the functionality of the FAT in persistent developmental stuttering we aim to extend the current knowledge about the involvement of this tract in speech production and contribute to the understanding of the newly described "motor stream" in language.

## Methods

### Participants

A total of 34 individuals participated in this study. Participants were physically healthy and reported no history of neurological disease or psychiatric disorder. They were all native Hebrew speakers who signed a written informed consent to participate in the study. The research protocol was approved by the Helsinki committee of the Tel-Aviv Sourasky Medical Center and by the ethics committee of the faculty of humanities in Bar-Ilan University.

Participants were assigned to the group of AWS based on the following criteria: (a) a reported history of stuttering since childhood, (b) exhibited a minimum of three stuttering-like disfluencies (SLD; Ambrose and Yairi 1999) per 100 syllables during an unstructured interview (described below) and (c) scored a total of at least 10 on the Stuttering Severity Instrument (SSI-III; Riley 1994). Assignment of participants to the control group was based on their self-report of having no history of stuttering.

To ensure that all participants assigned to the group of AWS were indeed individuals who stutter, two experienced speech pathologists (O.A. and R.E.-V.) were asked to blindly confirm the original classification based on their impression from the audio-visual recording of an unstructured interview (see "Speaking tasks" below). Classification was performed separately by each speech pathologist, and only those participants who were classified by both speech pathologists as individuals who stutter were assigned to the group of AWS. Based on these criteria, 15 participants were assigned to the group of AWS (3 females, mean age 32 years, age range 19–52 years), and 19 were assigned to the control group (3 females, mean age 33 years, age range 19–53 years). Table 1 presents the average demographic characteristics of the AWS and the control participants.

### Speaking tasks

To assess the frequency of stuttering, participants were evaluated during two speaking tasks: an unstructured interview and a reading task (Riley 1994).

#### *Unstructured interview*

Each participant was seated in a quiet room together with the experimenter (V.K.-D.), and was asked to talk for 10 min about a neutral topic, such as a recent travel experience, a movie or a book. The experimenter was instructed to refrain from interrupting the speaker, and to ask questions only when the participant was having difficulties finding a topic to talk about. The session was recorded simultaneously with a digital video camera (Sony DCR-DVD 106E, Sony Corporation of America, New York, NY, USA) and with a noise canceling microphone (Sennheiser PC21, Sennheiser Electronic Corporation, Berlin, Germany). Audio signals from the microphone were digitally recorded using audio processing software (Goldwave, Inc., St. John's, Canada), on a mono channel, with a sampling rate of 48 kHz (16 bit).

#### *Reading task*

Each participant was seated in a quiet room together with the experimenter and was asked to read aloud one of three paragraphs from the standardized and phonetically balanced Thousand Islands reading passage (Amir and Levine-Yundof 2013). The three paragraphs were of similar size (on average: 200 syllables) and the different paragraphs were assigned to the participants in a random order. This task was recorded using a video camera (see above).

### Evaluation of speech fluency

We obtained three measures of speech fluency: (a) Average speech rate, (b) Stuttering-like disfluencies (SLD) and (c) Percent of stuttered syllables. These measures were calculated based on the digital audio recordings of the unstructured interview. The audio recordings were used because of their superior auditory signal-to-noise ratio (SNR) compared to the video recordings, and based on reports that visual information does not improve the reliability of measuring stuttering frequency (MacDonald and Mallard 1979; Williams et al. 1963). To calculate the fluency measures, each interview was transcribed, until a minimum of 600 consecutive syllables was obtained (exact number of syllables slightly differed between participants as only complete sentences were analyzed). Disfluencies were first annotated by two independent trained research assistants and then re-evaluated by a speech pathologist (O.A.). There was a high level of agreement between the raters on the classification of disfluencies, but any cases of disagreement were discussed until full agreement between all raters was reached. To reduce potential bias, both the research assistants and the speech pathologist were blind to the participant's group assignment (stuttering/control).

The three measures of speech fluency (average speech rate, SLD, percent of stuttered syllables) were calculated as follows: (a) average speech rate was measured in units of syllables per second (SPS). It was calculated as the ratio between the total number of analyzed syllables and the time it took the participant to produce them. This measure was obtained from a visual and audio inspection of the spectrographic display of the speech signal (as discussed in Finkelstein and Amir 2013; Rochman and Amir 2013); (b) SLD was calculated as the number of part-word repetitions, monosyllabic-word repetitions and disrhythmic phonations, per 100 syllables. Other disfluencies like interjections, revisions or phrase repetitions were excluded from this measure (Ambrose and Yairi 1999); (c) the percent of stuttered syllables was calculated based on the syllables that included any type of SLD (Yairi and Ambrose 2005).

### Stuttering severity evaluation

We evaluated stuttering severity of each individual of the group of AWS by administering the stuttering severity evaluation instrument (Riley 1994). Following the administration protocol for adults, we evaluated the percent of stuttered syllables based on the transcription of the two speaking tasks (the unstructured interview and the reading task). Stuttering duration scores and physical concomitants were evaluated by two speech pathologists (O.A and R.E.-V.), based on the video recording of the speaking tasks. Taken together, the percent of stuttered syllables, stuttering duration scores and physical concomitants were used to obtain a total score of stuttering severity rate (SSI score).

### Image acquisition

Magnetic resonance imaging (MRI) was performed on a 3T General Electric MRI scanner at the Tel-Aviv Sourasky Medical Center. The MRI protocol included standard anatomical and diffusion imaging sequences, acquired with an eight channel head-coil. Participants were asked to lie still during the scan, and their head motion was minimized by placing cushions around their heads. Functional MRI experiments were also included in the scan protocol but those data are not reported here.

#### *T1 image acquisition*

High resolution T1 weighted anatomical images were acquired using a 3D fast spoiled gradient echo (FSPGR) sequence. We collected about 150 axial slices ($\pm 12$ slices), covering the entire cerebrum, with a spatial resolution of $1 \times 1 \times 1$ mm voxel size.

#### *Diffusion weighted image acquisition*

A standard DTI protocol was applied by means of a single-shot spin-echo diffusion-weighted echo-planar imaging (DW-EPI) sequence. We collected $\sim 68$ axial slices, adjusting the number of slices to cover the entire cerebrum in each participant (FOV = 240 mm; $128 \times 128$ matrix; 2 mm thick axial slices; voxel size: $\sim 2 \times 2 \times 2$ mm). 19 diffusion-weighted volumes ($b = 1{,}000$ s/mm$^2$) and one reference volume ($b = 0$ s/mm$^2$) were acquired using a standard direction matrix (e.g., Sasson et al. 2010, 2012, 2013). This protocol was repeated twice for an improved signal-to-noise ratio. Scan repetitions were not averaged so that tensors were fit to the entire dataset from both scans (see "Data preprocessing"). Scanning 19 directions twice was motivated by the fact that short scan time (5:50 min per scan) reduces the chances of within-scan motion while maintaining robust anisotropy measurements (Jones 2004).

### Software

All data analysis and statistics were performed using Matlab 2012b (The Mathworks, Nattick, MA, USA). For data preprocessing, we used the 'mrDiffusion' package (http://white.stanford.edu/newlm/index.php/Software). Tract identification and quantification were executed using 'AFQ', an automated segmentation tool (Yeatman et al. 2012).Visual inspection of the tracts and manual cleaning was performed

via 'Quench', an interactive 3D visualization tool (Akers 2006; http://white.stanford.edu/newlm/index.php/Software#QUENCH).

## Data preprocessing

As a first step, T1 images were aligned to the AC–PC orientation. Diffusion weighted images were corrected for Eddy-current distortions and subject motion (Rhode et al. 2004). Each diffusion weighted image was registered to the mean of the two non-diffusion weighted (b0) images and the mean b0 image was registered automatically to the T1 image, using a rigid body mutual information maximization algorithm (implemented in SPM5; Friston and Ashburner 2004). Then, the combined transform resulting from motion correction, eddy current correction and anatomical alignment was applied to the raw diffusion data once, and the data was resampled at exactly $2 \times 2 \times 2$ mm isotropic voxels. By applying the combined transform, we achieved AC–PC aligned T1 registered images while only resampling the raw data once. Next, the table of gradient directions was appropriately adjusted to fit the resampled diffusion data (Leemans and Jones 2009).

We fitted the raw diffusion data with the tensor model using a standard least-squares algorithm. Then, we extracted the eigenvectors and eigenvalues of the tensor and calculated FA as the normalized standard deviation of the eigenvalues (Basser and Pierpaoli 1996). Using the eigenvalues, we also calculated mean diffusivity (MD) as the average of all three eigenvalues. Axial diffusivity (AD) and radial diffusivity (RD) were calculated as complementary measures and were respectively defined as the diffusivity along the principal axis (AD) and as the average diffusivity along the two remaining minor axes (RD).

## Tract identification protocol

We identified the FAT and the CST in each participant's left and right hemispheres. To identify these tracts we used a procedure composed of three steps: (1) whole brain fiber tractography (2) region-of-interest (ROI) based fiber tract segmentation and (3) fiber tract cleaning.

### *Step 1: whole brain fiber tractography*

Whole brain fibers were tracked in the native space of each participant using a deterministic streamlines tracking algorithm (Basser et al. 2000; Mori et al. 1999) with a fourth-order Runge–Kutta path integration method (1 mm fixed step size, 8 seed points per voxel). The tracking algorithm was seeded with a white matter mask of all voxels with FA greater than 0.2 and tracking was halted when FA dropped below 0.15 or if the angle between the last and the next step direction was greater than 30° (Dougherty et al. 2007). Minimum streamline length was set to 20 mm.

### *Step 2: fiber tract segmentation*

We used a multiple ROI approach to delineate the tracts in each participant. To segment the fibers, the whole brain fiber group (obtained in step 1) was intersected with these ROIs using logical operations (AND, NOT). Below we describe the protocol used to identify the ROIs of the FAT and the CST.

#### *FAT*

We propose a protocol for identifying the FAT that is based on several previous studies (Catani et al. 2012; Ford et al. 2010; Lawes et al. 2008). Figure 1 illustrates this protocol in an attempt to promote common practices in future studies of this tract.

Two ROIs were defined on the Montreal Neurological Institute (MNI) template (ICBM 2009a Nonlinear Asymmetric template; Fonov et al. 2011). The first ROI was defined on a sagittal slice at the level of $x = 45$ (for the right tract) or $x = -45$ (for the left tract; see Fig. 1b, right image). This ROI (IFG) included all voxels above the Sylvian fissure and below the inferior frontal sulcus. Anteriorly, it was bounded by a coronal slice at the anterior end of the pars triangularis as it is seen on sagittal slices $x = \pm 45$. Posteriorly, it was bordered by a coronal slice at the most ventral end of the precentral sulcus as it is seen on the same sagittal slices ($x = \pm 45$). The second ROI was defined on axial slice $z = 45$ (see Fig. 1b, left image). This ROI (SMA/pre-SMA), encompassed a rectangle that was medially bordered by the mid-sagittal plane; laterally, it was bordered by a sagittal plane at the most medial point where the precentral sulcus is still seen on $z = 45$. Anteriorly, this ROI was bordered by a coronal slice at the level of the anterior portion of the genu of the corpus callosum and posteriorly, it was bordered by a coronal slice at the level of the precentral sulcus defined on the mid-sagittal plane.

These four ROIs (left and right IFG, left and right SMA/pre-SMA) were back transformed into an individual's native space based on a non-linear transformation calculated between each individual's volume anatomy and the MNI template (as implemented in Yeatman et al. 2012). The whole brain fiber group was intersected with the transformed left ROIs (left IFG, left SMA/pre-SMA) to obtain the left tract and with the right transformed ROIs (right IFG, right SMA/pre-SMA) to obtain the right tract.

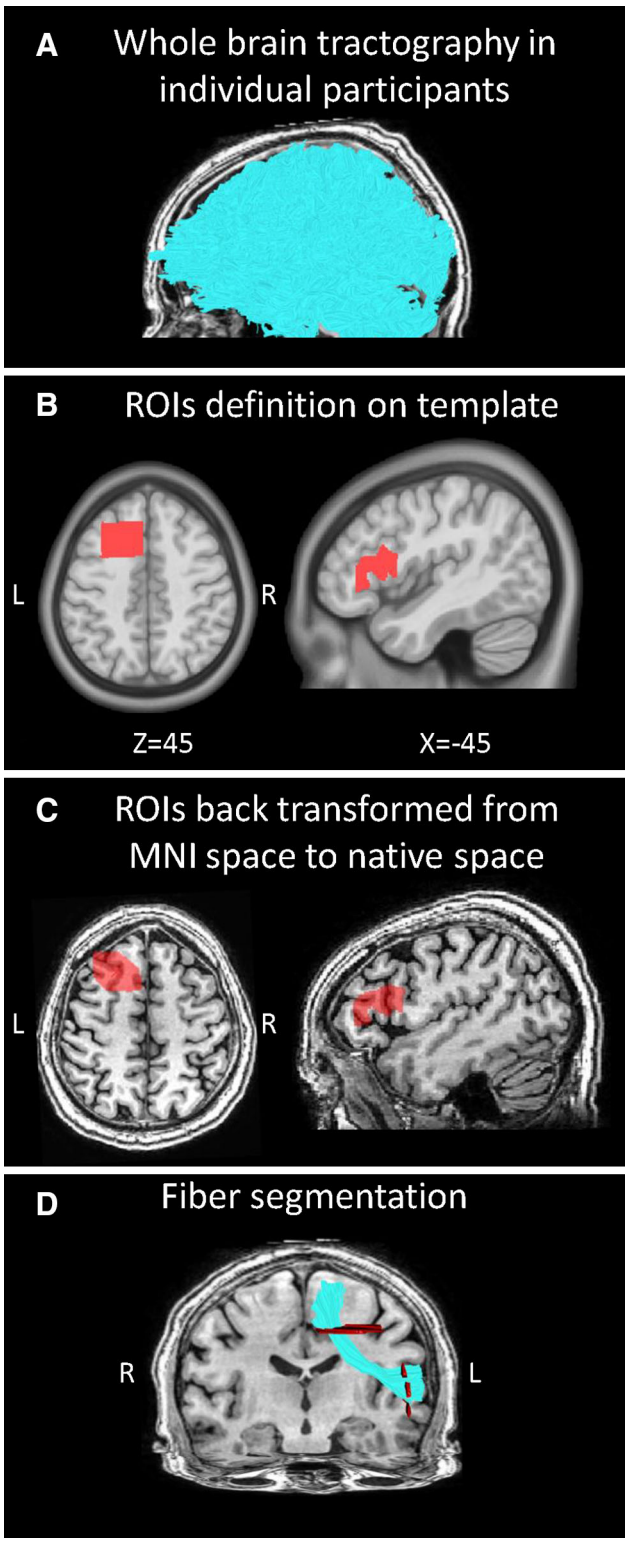


◀**Fig. 1** FAT identification protocol. **a** Whole brain fiber tractography is overlaid on a sagittal T1 image of a representative participant. **b** ROIs (in *red*) are defined on the MNI template (ICBM 2009a Nonlinear Asymmetric; Fonov et al. 2011). The left IFG ROI is overlaid on a sagittal image and the left SMA/pre-SMA ROI is overlaid on an axial image. **c** The left hemisphere ROIs are shown after they were back transformed from the MNI space to the native space of an individual participant. **d** The left FAT resulting from the intersection of the whole brain fiber group (illustrated in **a**) with the back transformed ROIs (shown in **c**). The tract is displayed in a 3D view, with coronal and axial images added for orientation. *FAT* frontal aslant tract, *IFG* inferior frontal gyrus, *SMA* supplementary motor area, *MNI* Montreal neurological institute

*CST*

The identification of the CST was based on a standard protocol by Wakana and colleagues (2007). All ROIs necessary for the tract identification were anatomically defined in every participant (by V.K.-D.). The first ROI encompassed the cerebral peduncle, marked on an axial plane at the level of the decussation of the superior cerebellar peduncle (see Figure 4 of Wakana et al. 2007). To define the second ROI, we visually inspected the tract that resulted from the intersection of the whole brain fiber group (step 1) with the first ROI. The second ROI was then drawn around the fibers that project to the primary motor cortex, as identified on the most ventral axial slice where the branching of the central sulcus is seen (see Figure 4 of Wakana et al. 2007). The whole brain fiber group was intersected with the left ROIs to obtain the left tract and with the right ROIs to obtain the right tract. As a final step, a logical NOT operation was applied on the resulting tracts with an ROI that covers the whole mid-sagittal plane. This last step was aimed to exclude all tracts that cross the midline via the pontine crossing fibers (Wakana et al. 2007).

*Step 3: fiber tract cleaning*

To remove outlier tracts, we used an automated cleaning procedure that removed fibers extending over 4 standard deviations from the mean fiber length or spatially deviating more than 5 standard deviations from the core of the tract (see Yeatman et al. 2012 for further details). Next, we manually inspected all the tracts in each individual using a gesture-based interface ('Quench', see "Software") and excluded single fibers that clearly did not fit the tract definition. For example, in the FAT we removed tracts that did not reach the IFG and in the CST we removed tracts that reached primary sensory (rather than motor) cortex.

To make sure that this manual cleaning phase was not biased, we calculated the ratio between the number of streamlines that were manually excluded from the fibers and the number of streamlines that were found in the original tract (i.e. before cleaning). These exclusion ratios were then compared between AWS and controls using two-tailed *t* tests with unequal variance (see "Results" and Figure S1).

## Evaluation of FAT endpoints

To calculate the MNI coordinates of the FAT endpoints for each participant, we first calculated a nonlinear transformation between the T1 volume anatomy of the participant and the MNI T1-template, using the mutual information maximization algorithm implemented in SPM5 (Friston and Ashburner 2004). We then applied the inverse transformation to assign an MNI coordinate to each voxel in the participants' native space. The centers of mass of the medial and lateral FAT endpoints were calculated for each participant, and their MNI coordinates were averaged across participants. We then used the automated anatomical labeling (AAL) atlas (Tzourio-Mazoyer et al. 2002) to assign anatomical labels to the average MNI coordinates of the medial and lateral FAT endpoints.

## Fiber tract quantification and group comparisons

### *Tract diffusivity measures*

For each participant and each tract, tract-FA and tract-MD measures were calculated as the average FA and MD across all voxels covered by the tract, respectively. These diffusion measures were compared between the groups using two-tailed *t* tests with unequal variance. Following up on these analyses, tract-AD and tract-RD were computed and compared between the groups in a similar fashion. Significance was corrected for 16 comparisons (4 tracts × 4 diffusion measures) using the false discovery rate (FDR) correction (Benjamini and Hochberg 1995), with alpha set at 0.05. To partial out the effect of age, all four diffusion measures were entered into ANCOVAs (analysis of covariance), with Age as a covariate.

### *Volume estimation*

The volume of each tract was estimated as the number of voxels covered by one streamline or more. This volume estimation was divided by the volume estimation of the whole brain fiber group (that was obtained by applying the same procedure to the whole brain fiber group). This normalization process was aimed to assure that differences in tract volume do not reflect a general difference in white matter volume between the groups.

Normalized volume estimates were compared between the groups using two-tailed *t* tests with unequal variance. The FDR was controlled based on the number of tracts with alpha set at 0.05.

### *Lateralization indices*

Three lateralization indices (LI) were computed for the FAT and CST, comparing volume estimates, FA and MD measures of the left and right tracts. For example, the volume lateralization index (VOL_LI) of the FAT was calculated based on the volume estimates of the left FAT ($VOL_{L\_FAT}$) and the volume estimate of the right FAT ($VOL_{R\_FAT}$) using the following equation:

$$VOL\_LI_{FAT} = (VOL_{L\_FAT} - VOL_{R\_FAT})/(VOL_{L\_FAT} + VOL_{R\_FAT})$$

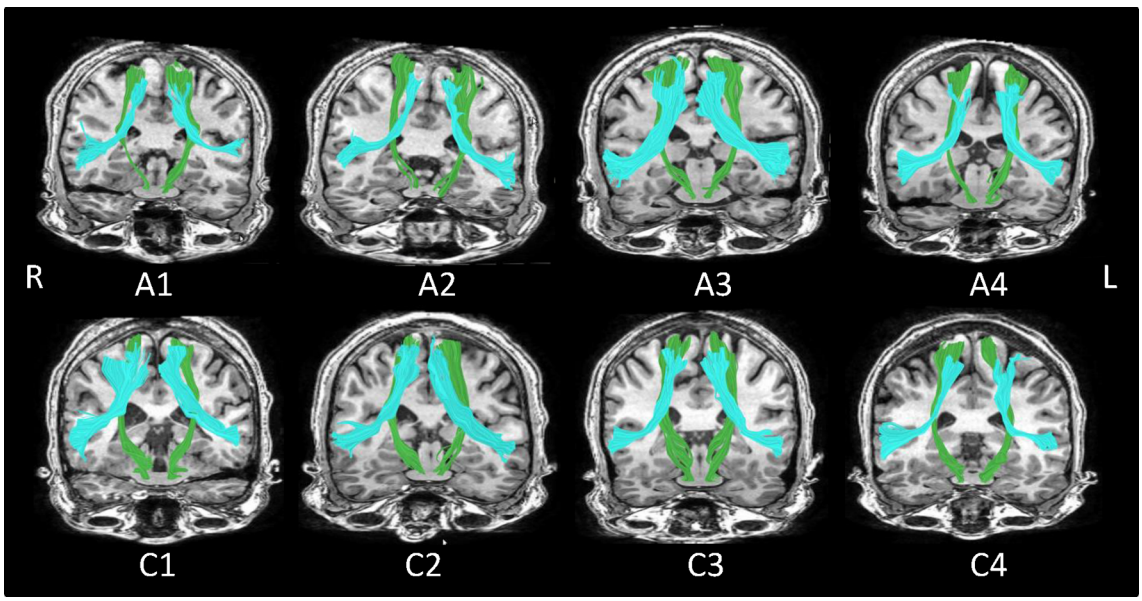


**Fig. 2** Bilateral FAT (*cyan*) and bilateral CST (*green*) shown in eight representative individuals. Tracts are displayed in a 3D view, with coronal and axial images added for orientation. *Top row* shows four AWS (**a1**–**a4**) and *bottom row* shows four control participants (**c1**–**c4**). *AWS* adults who stutter, *FAT* frontal aslant tract, *CST* corticospinal tract

The lateralization indices were compared between the groups using two-tailed *t* tests with unequal variance while controlling the FDR based on the number of tracts with alpha set at 0.05.

### *FA profiles along the tract*

FA and MD profiles of each tract were obtained by sampling the full length of the tract at 100 equi-spaced nodes and calculating FA and MD in each node as a weighted average across the streamlines of that tract (Yeatman et al. 2012). Profiles were calculated along the entire length of the tracts, i.e. between the cortical endpoints of the tracts.

FA and MD profiles were compared between the groups using multiple two-tailed *t* tests. A permutation-based multiple comparisons correction (Nichols and Holmes 2002) was used to calculate the critical cluster of adjacent significant *t* tests. Significance was corrected for 400 comparisons (4 tracts × 100 nodes in each tract) setting the corrected alpha to 0.05. We report clusters of nodes in which (1) all neighboring nodes significantly differed between the groups at the level of 0.05 (uncorrected) and (2) the cluster of significant values was larger than the critical cluster size (Nichols and Holmes 2002; Yeatman et al. 2012).

### Brain–behavior correlations

In clusters showing a significant group difference, we further aimed to examine how individual variability in tract properties predicts behavioral properties. To this end, we extracted diffusivity measures from the clusters of nodes that significantly differed between the groups, and then analyzed the correlation between diffusivity measure and speech fluency within the group of AWS and the group of controls separately.

To calculate a correlation measure, we had to reduce the dimensionality of the tract profile into a single diffusivity measure. This was done by extracting MD measures from a fixed sized window within the cluster of nodes where significant differences were found and averaging the MD values measured within this window. The size of the window was arbitrarily set to 11 nodes that include the middle-most node and 5 additional nodes on each side. We further validated that the results were not specific to a window size of 11 nodes by replicating the correlation analyses with different window sizes (see Figure S4).

Speech fluency was assessed using the speech rate (measured in SPS). This specific measure was chosen for its proximity to the fluency measure used by Catani et al. (2013) in their study of the FAT in primary progressive aphasia.

We calculated Spearman's rank-order correlations to assess the link between an individual's diffusion data and their speech rate. Spearman correlations were used due to evidence for non-normal distribution of both MD and speech rate as indicated by the Kolmogorov–Smirnoff test (Corder and Foreman 2009). Importantly, the correlations were calculated separately for AWS and controls, to avoid spurious correlations caused by the significant group differences found in both MD and in SPS. Fisher's *Z* transformations were used to assess the significance of the difference between the correlation coefficients measured in AWS and control participants (Sheskin 2003). Finally, partial Spearman correlations were calculated between MD and SPS within each group, controlling for the effect of Age. This latter analysis served to confirm that the correlation effects are not driven by the large age range in our sample.

## Results

### Behavioral results

Participants in the group of AWS scored an average SSI score of 24.07 (standard deviation 7.38, range 10–41.5). The wide range of SSI scores demonstrated that this group consisted of different degrees of symptoms, ranging from very mild to very severe. Specifically, one participant was rated as exhibiting very mild stuttering, one mild, eight moderate, four severe and one very severe. On average, AWS and controls were of similar age and had similar handedness and education levels (see Table 1). As expected, the groups differed significantly in all three measures of speech fluency (speech rate: $t(32) = 3.71$, $p < 10^{-3}$, SLD: $t(32) = 2.66$, $p < 0.05$, percent of stuttered syllables: $t(32) = 6.14$, $p < 10^{-6}$, see Table 1).

Spearman's rank-order correlations between speech rate (in SPS) and all the other measures used for the assessment of speech fluency and stuttering severity (SLD, % stuttered syllables, SSI score) showed a significant negative correlation in AWS (SPS-SLD: $r_s = -0.72$, $p < 0.005$; SPS-percent stuttered syllables: $r_s = -0.68$, $p < 0.01$; SPS-SSI score: $r_s = -0.6$, $p < 0.05$).

### Tract identification

The left FAT and the bilateral CST were identified successfully in all participants ($N = 34$). The right FAT was identified in 33 of the 34 participants, but could not be traced in one AWS. Figure 2 shows the tracts of interest identified in eight representative participants (four participants of each group). Figure 3 zooms in on the endpoints of the left FAT in a subset of these participants. As is evident in these figures, the FAT connects medial and lateral frontal cortices.

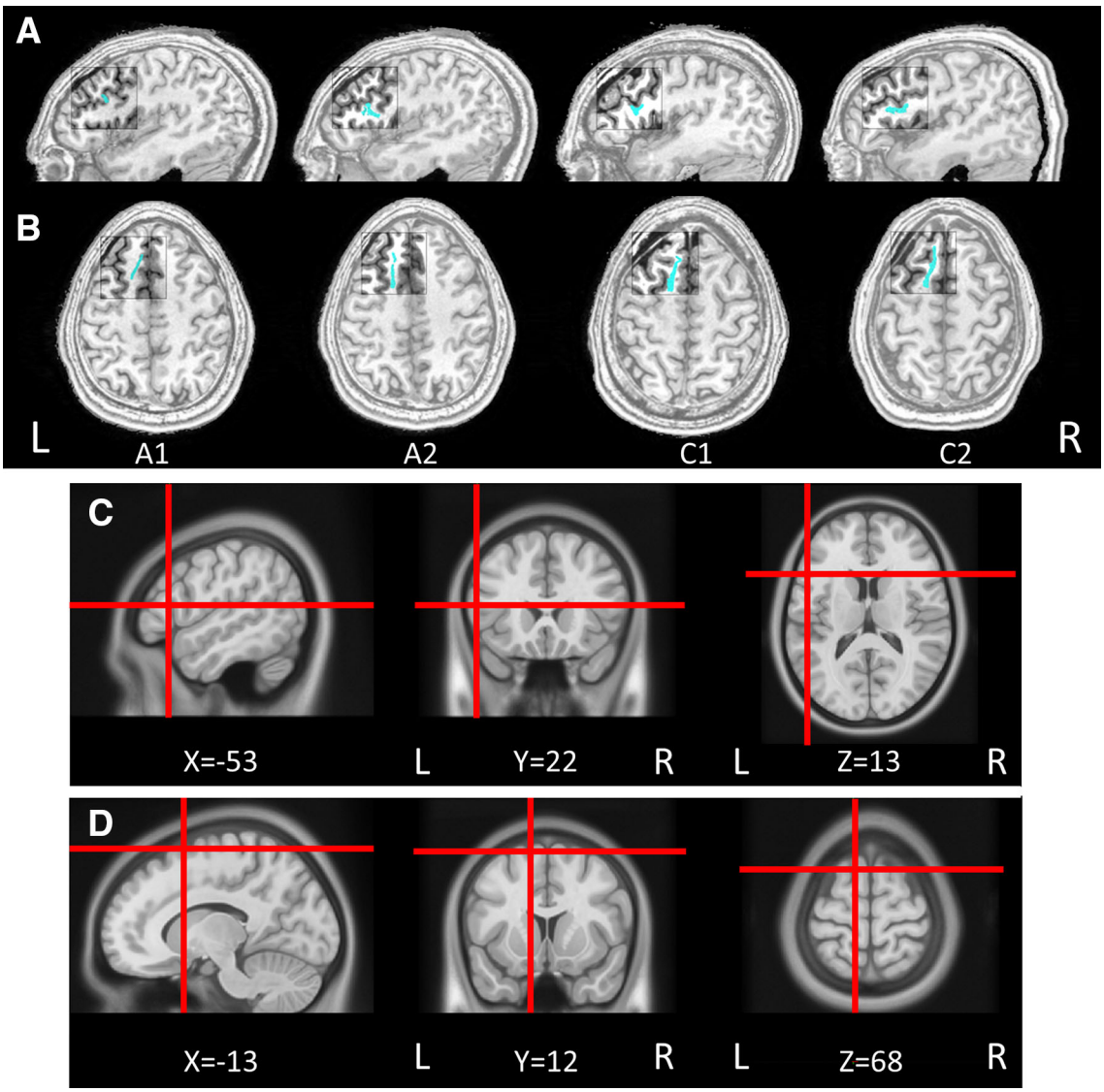


**Fig. 3** The FAT endpoints. The projections of the left FAT (*cyan*) are shown in four representative participants (individuals a1, a2, c1 and c2 of Fig. 2). The lateral projections are overlaid on sagittal T1 images (**a**) and the medial projections are overlaid on axial T1 images (**b**). For illustration purposes, the tracts are surrounded by *squares* and the data *outside* the *squares* is slightly dampened. The mean lateral (**c**) and medial (**d**) MNI coordinates of the left FAT endpoints are shown on an MNI template (ICBM 2009a Nonlinear Asymmetric template; Fonov et al. 2011)

In a further analysis, we calculated the mean MNI coordinates of the center of mass of the FAT endpoints across all participants. We used the automated anatomical labeling (AAL) atlas (Tzourio-Mazoyer et al. 2002) to assign anatomical labels to these endpoints. This procedure revealed that in our sample, the FAT terminates medially in the SMA/pre-SMA (the AAL atlas includes both regions under the label SMA) or in the adjacent superior frontal gyrus (MNI coordinates [−13, 12, 68] [14, 12, 70]). Laterally, the FAT terminates in the pars triangularis of the inferior frontal gyrus (MNI coordinates [−53, 22, 13] and [56, 23, 15]).

The exclusion ratios that indicate the relative number of streamlines excluded during manual cleaning stage (see "Methods") showed no significant difference between the groups ($p > 0.1$; Figure S1).

## Elevated mean diffusivity in bilateral frontal aslant tracts of AWS compared with controls

For each tract, we compared FA and MD values of the AWS and control participants averaged across the entire tract (termed tract-FA and tract-MD, respectively). This analysis revealed that AWS have higher tract-MD values in

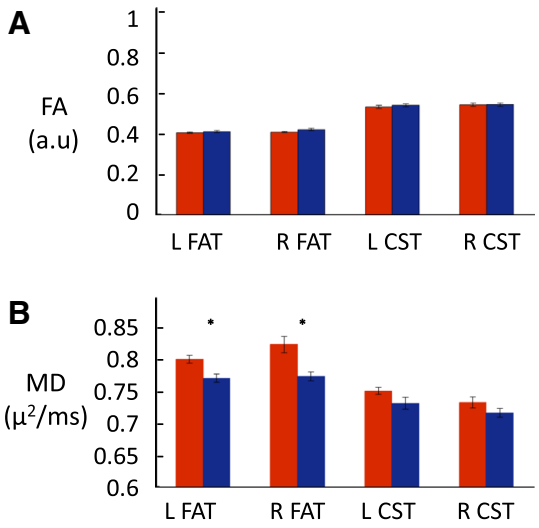


**Fig. 4** Group comparison of tract-FA and tract-MD values. Average FA (**a**) and MD (**b**) values measured in bilateral FAT and bilateral CST are shown in AWS (*red*) and in controls (*blue*), with *error bars* denoting ±1 standard error of the mean. *Asterisks* denote significant group differences after controlling for the FDR with alpha set at 0.05 (see the main text for further details). Significant increase in MD is observed in bilateral FAT of AWS compared with controls. Note that FA and MD values are measured in different units, hence the difference in the *y* axis range of **a** and **b.** *AWS* adults who stutter, *FAT* frontal aslant tract, *CST* corticospinal tract, *L* left, *R* right, *FA* fractional anisotropy, *MD* mean diffusivity, *FDR* false discovery rate, *a.u.* arbitrary units, *ms* millisecond

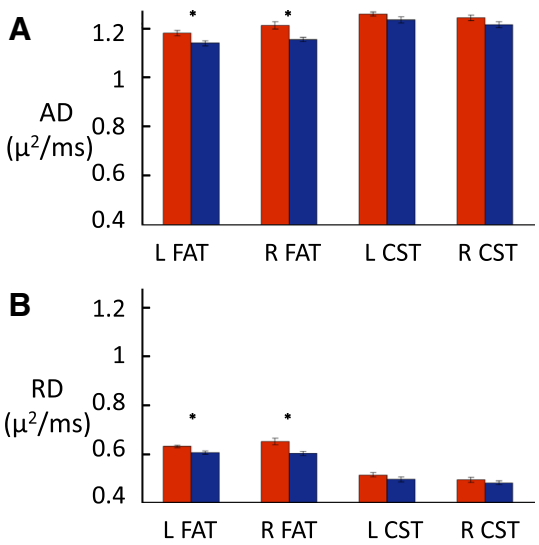


**Fig. 5** Group comparison of tract-AD and tract-RD values. Average AD (**a**) and RD (**b**) values measured in bilateral FAT and bilateral CST are shown in AWS (*red*) and in controls (*blue*), with error bars denoting ±1 standard error of the mean. *Asterisks* denote significant group differences after controlling for the FDR at alpha level = 0.05 (see the main text for further details). Significant increase in both AD and RD are observed in bilateral FAT of AWS compared with controls. *AWS* adults who stutter, *FAT* frontal aslant tract, *CST* corticospinal tract, *L* left, *R* right, *AD* axial diffusivity, *RD* radial diffusivity, *FDR* false discovery rate, *ms* millisecond

bilateral FAT compared with fluent controls (Fig. 4b, left FAT: $t(32) = 3.24$, $p < 0.005$; right FAT: $t(31) = 3.55$, $p < 0.005$; both effects were significant when controlling the FDR with alpha set at 0.05). No significant group differences were found in average tract-MD of the bilateral CST ($p > 0.1$) and similarly, no significant differences were observed in average tract-FA values of either tract ($p > 0.09$, Fig. 4a).

To further identify the source of the group differences in tract-MD, we followed up on these results with a comparison of tract-AD and tract-RD values (Fig. 5). We found that both AD and RD extracted from bilateral FAT are increased in AWS compared with controls (AD in left FAT: $t(32) = 2.68$, $p < 0.05$; AD in right FAT: $t(31) = 3.38$, $p < 0.005$; RD in left FAT: $t(32) = 3$, $p < 0.01$, RD in right FAT: $t(31) = 3.26$, $p < 0.005$; both effects were significant when controlling the FDR with alpha set at 0.05).

Altogether, 16 group comparisons were conducted in this analysis (4 tracts × 4 diffusion measures). All the reported group differences in tract-MD, tract-AD and tract-RD of bilateral FAT were significant when controlling the FDR for 16 comparisons with alpha set at 0.05.

To partial out the effect of age on the results, we entered each diffusion measure into an ANCOVA, with Age as a covariate. The results show that in MD, AD and RD, the effects of Group remain significant after controlling for Age and that there is no significant Group by Age interaction. In FA, no significant Group effect and no significant Group by Age interaction is found (see Table 2).

**Table 2** ANCOVA test results

| | Group effect | | Group × age interaction | |
|---|---|---|---|---|
| | *F* | *P* | *F* | *P* |
| Left FAT[a] | | | | |
| FA | 0.59 | >0.4 | 0.87 | >0.4 |
| MD | 11.48 | <0.05* | 1.56 | >0.2 |
| AD | 7.54 | <0.05* | 3.06 | >0.05 |
| RD | 10.24 | <0.01* | 0.26 | >0.6 |
| Right FAT[b] | | | | |
| FA | 3.17 | >0.05 | 1.6 | >0.2 |
| MD | 12.6 | <0.01* | 0.78 | >0.5 |
| AD | 11.91 | <0.01* | 3.72 | >0.05 |
| RD | 10.8 | <0.01* | 0.05 | >0.8 |

*ANCOVA* analysis of covariance, *FAT* frontal aslant tract

* Significant differences after controlling the FDR for 16 comparisons with alpha set at 0.05

[a] In left FAT, Degrees of freedom = 30

[b] In right FAT, Degrees of freedom = 29

### Similar tract volumes and lateralization indices in AWS and in fluent controls

Comparing the normalized volumes of the tracts did not reveal any significant group differences ($p > 0.1$). Similarly, no significant group differences were found in the LIs calculated over volume estimations, FA and MD measures ($p > 0.09$). The mean LIs measured in the CST and in the FAT were close to zero in both groups, with absolute mean LI values below 0.1, indicating bilaterality.

### Increased mean diffusivity observed along the left tract profiles

Differences in diffusion measures between the groups may be masked in the averaged tract-diffusivity estimates, due to large variability along the length of the tract (Yeatman et al. 2011). We therefore, generated profiles describing FA and MD along the tracts and then compared the profiles between the groups using multiple *t* tests and a permutation based multiple comparison correction (Nichols and Holmes 2002; Yeatman et al. 2012 and see "Methods" of this paper).

This analysis showed that MD values measured in AWS are significantly higher than those measured in fluent controls, in a large cluster of nodes measured within the left FAT (Fig. 6a, cluster ranges across nodes 55–90) as well as in a large cluster of nodes measured within the left CST (Fig. 6b, cluster ranges across nodes 74–97). In the right FAT and in the right CST we did not find any cluster of nodes that significantly differed between the groups and was large enough to survive the multiple comparison

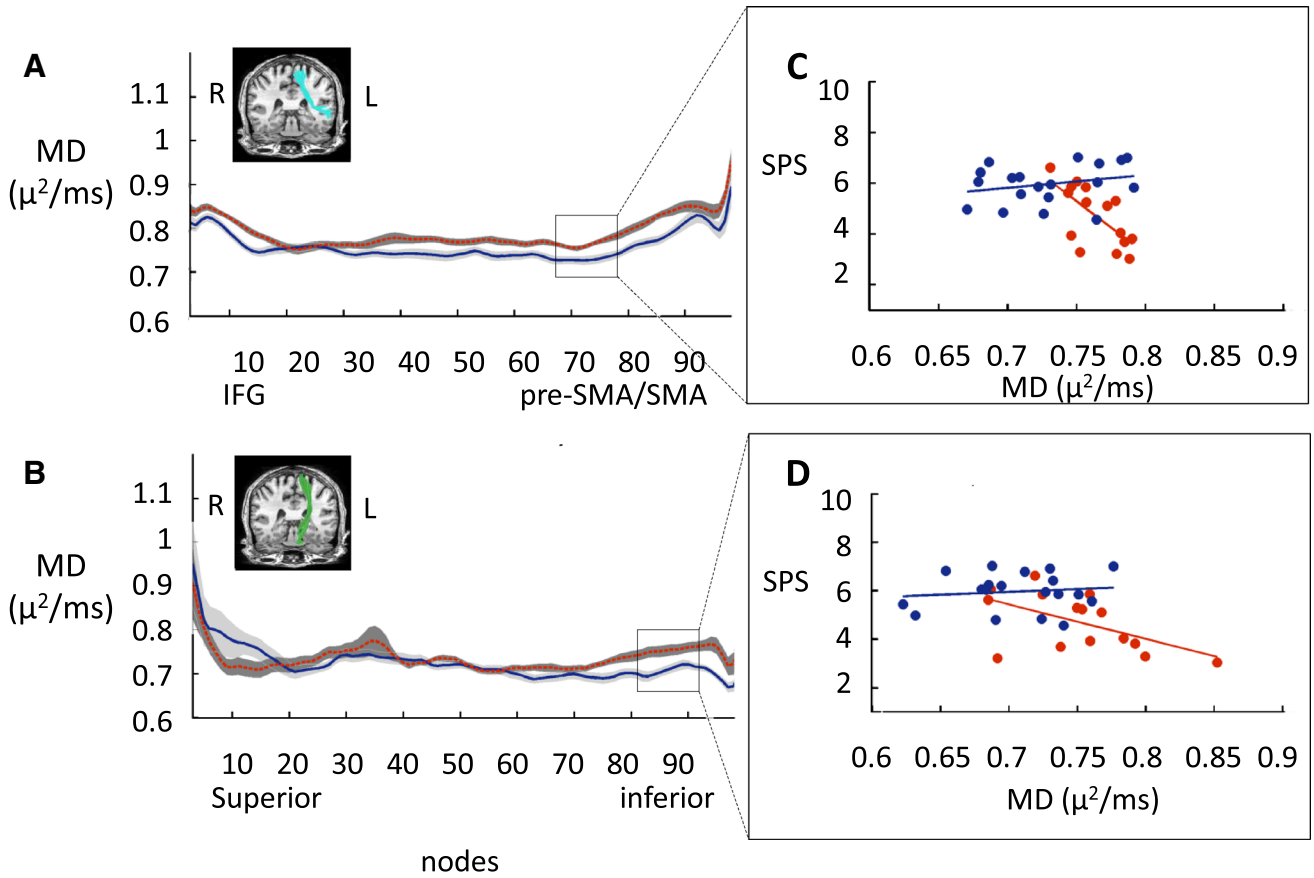


**Fig. 6** Group comparison of MD profiles and brain-behavior correlations. MD profiles are shown for the left FAT (**a**) and the left CST (**b**). The *colored line* indicates the average profile of the AWS (*red*) and controls (*blue*), with *grey regions* denoting ±1 standard error of the mean (AWS: *dark grey*; controls: *light grey*). Significant group-differences between the profiles are observed in nodes 55–90 of the left FAT and in nodes 74–97 of the left CST (see text). *Rectangles* overlaid on the profiles represent fixed sized windows centered around the midpoint of the significant cluster of nodes (11 nodes in each window). In **c** and **d**, MD values of individual participants measured within these windows are plotted against their SPS. In the left FAT (**c**), data show that MD is negatively correlated with speech rate (measured in SPS) in AWS (*red*; $r_s = -0.7$, $p < 0.005$) but not in controls (*blue*; $r_s = 0.19$, $p > 0.4$). No significant correlation is found in the left CST (**d**) (in AWS: $r_s = -0.56$, $p = \sim 0.03$, in controls $r_s = 0.005$, $p > 0.9$). Note that a trend is observed in the CST of AWS, yet it does not reach significance after correcting for multiple comparisons (see "Methods"). *AWS* adults who stutter, *FAT* frontal aslant tract, *CST* corticospinal tract, *MD* mean diffusivity, *ms* millisecond, *IFG* inferior frontal gyrus and *SMA* supplementary motor area

cluster-based threshold that was used (Figure S2). In addition, no significant difference was found between the FA profiles of AWS and controls along any of the tracts (Figure S3).

### Mean diffusivity within the left FAT negatively correlates with speech fluency in AWS

To establish the functional contribution of the left FAT and the left CST in AWS, we measured brain-behavior correlations between the MD values measured within these tracts and the speech rates. For each participant, we extracted a single measure of MD from a fixed size window located within the cluster of nodes where the groups significantly differed (see "Methods"). We correlated the resulting MD value of each participant with their speech rate (estimated using SPS). To avoid spurious correlations caused by the significant group differences found in both MD and SPS separately, Spearman correlations were calculated separately for AWS and controls (altogether, four correlations were computed: 2 groups × 2 tracts).

Results show that in the left FAT, higher MD values predict lower SPS in AWS ($r_s = -0.7$, $p < 0.005$; FDR corrected for four comparisons with alpha set to 0.05) but not in controls ($r_s = 0.19$, $p > 0.4$). Importantly, the correlation coefficients calculated in the two groups differ significantly (Fisher's $Z = 2.77$, $p < 0.01$), and a partial correlation analysis revealed that the negative correlation observed in the left FAT of AWS remains significant after controlling for Age ($p < 0.001$, FDR corrected for four comparisons with alpha set to 0.05). No significant correlation is found in the left CST of both groups (in AWS: $r_s = -0.56$, $p = \sim 0.03$, in controls: $r_s = 0.005$, $p > 0.9$). Notably, in the CST of AWS, a trend is observed, however it does not reach significance following the control for FDR.

To evaluate the stability of these correlations, we modified the size of the window used for MD extraction and we measured the Spearman correlation coefficients obtained using different window sizes (Figure S4). This analysis showed a stable pattern of results, verifying that the pattern of correlations between MD and speech rate does not depend on the particular window size used in the main analysis. Specifically, the results did not change when we used the entire cluster of nodes that significantly differed between the groups in the tract profile analysis (nodes 55–90 of the left FAT, nodes 74–97 of the left CST). Within these clusters, MD-SPS correlations were significant in AWS ($r_s = -0.65$, $p < 0.05$; FDR corrected for four comparisons with alpha set to 0.05) but not in controls ($r_s = 0.01$, $p > 0.97$). The correlation coefficients differed significantly between the groups (Fisher's $Z = 2.04$, $p < 0.05$), and the negative correlation observed in the left FAT of AWS remained significant after controlling for Age using a partial correlation analysis ($p < 0.05$). In addition, no significant correlation was found in the left CST of both groups (in AWS: $r_s = -0.53$, $p = \sim 0.04$, in controls: $r_s = -0.14$, $p > 0.5$). Similar to the main analysis (of 11 nodes), a trend was observed in the left CST of AWS, yet it did not reach significance following the control for FDR.

## Discussion

Our results show that the bilateral FAT is involved in speech production in a clinical population of individuals with persistent developmental stuttering. Specifically, we show that the microstructural properties of this tract, assessed using mean diffusivity, significantly differ between individuals who stutter and fluent controls. Beyond group comparisons, our data further show that the mean diffusivity calculated within the left FAT predicts individual speech rate in individuals who stutter. By demonstrating the involvement of the FAT in a developmental disorder that disrupts speech fluency, our results strengthen the view that the FAT plays a role in speech production, possibly via a "language motor stream" (Dick et al. 2013).

Our data show that AWS have higher MD values in the left FAT compared with controls. Further, the MD values calculated within this tract negatively correlate with the speech rate measured in individuals who stutter: the lower the MD, the higher the speech rate (and the closer it is to the average speech rate measured in controls). While these results demonstrate brain-behavior correlations with MD in the left FAT, the previous analysis of functional correlations within the left FAT in primary progressive aphasia (Catani et al. 2013) showed a negative correlation between speech fluency and RD values (along with a positive correlation between speech fluency and FA values). MD and RD values typically correlate in a positive fashion (see Figure 6 of De Santis et al. 2014). Thus, it appears that despite the different diffusion measures and the different assessment tools used for measuring fluency, both studies imply that less restriction on water diffusion within the left FAT is associated with a lower degree of fluency. By showing that this brain-behavior correlation is unique to AWS and does not hold in controls, our findings suggest that the left FAT may be an important predictor of fluency in clinical populations, but not necessarily in the neurotypical population.

In the right FAT, our data show a significant group difference in the average MD of the entire tract with no significant difference in the profile analysis. Specifically, the profile analysis of the right FAT shows several clusters of nodes that differ between the groups, yet none of these clusters is large enough to survive the cluster-based

multiple comparison correction that we apply (see "Methods"). This suggests that differences in MD values of the right FAT are equally spread in multiple (not necessarily neighboring) points along the right FAT.

In light of the persistent developmental stuttering literature, our findings in *bilateral* FAT are not surprising. The involvement of both hemispheres in the etiology of stuttering has long been proposed (Kushner 2012; Travis 1931) and many functional imaging studies continue to indicate the contribution of both hemispheres to developmental stuttering (Biermann-Ruben et al. 2005; Brown et al. 2005; Chang et al. 2009; Kell et al. 2009; Lu et al. 2010a; Watkins et al. 2008; Xuan et al. 2012). Structural imaging studies of white matter in developmental stuttering have, for the most part, highlighted left frontal white matter abnormalities as the core deficit in the disorder (Chang et al. 2008; Cykowski et al. 2010; Sommer et al. 2002; Watkins et al. 2008). However, some of these studies also point to stuttering-related white matter differences in the right hemisphere (Chang et al. 2008, 2010; Connally et al. 2013; Watkins et al. 2008). Our findings are consistent with the view that both hemispheres contribute to fluent speech production in individuals who stutter, as well as with the general proposal that the underlying mechanisms required for speech production (like sensory-motor transformation) occur bilaterally (Cogan et al. 2014).

One view of persistent developmental stuttering maintains that the core deficit is left hemispheric (Chang et al. 2008; Kell et al. 2009), while the right hemisphere is recruited to compensate for the left hemisphere impairment (Preibisch et al. 2003). However, while some authors suggest that the right hemisphere involvement is beneficial, i.e., enhances fluency (Braun et al. 1997; Kell et al. 2009; Preibisch et al. 2003) others suggest that it is not (Brown et al. 2005; Chang et al. 2010; Foundas et al. 2004; Fox et al. 2000; Moore 1984). Our data show the same pattern of results (MD elevation in AWS compared with controls) in both the left and right FAT, which is difficult to reconcile with the idea that the right tract is compensating for the left impairment. However, because all participants of this study were adults, we cannot be conclusive about the functional interpretation of the differences that we find. All the observed differences can equally constitute the cause for stuttering or reflect compensation processes following years of stuttering.

We originally examined the FAT in the context of persistent developmental stuttering based on its recent depiction as a language production pathway (Dick et al. 2013). However, in fMRI, functional connectivity between medial-dorsal and ventral-lateral frontal regions has been related to domain general error monitoring (Dosenbach et al. 2006; Eckert et al. 2009; Vaden et al. 2013). This "cingulo-opercular network" has been proposed to relay information between the dorsal paracingulate/anterior cingulate cortex and the lateral anterior insula. While these regions do not overlap precisely with the endpoints of the FAT (Fig. 3, see also Catani et al. 2012), it is still possible that the FAT takes part in relaying information related to error monitoring in speech production. We offer this possibility here because, first, it is well-known that fiber tracking algorithms are prone to errors near the gray matter, where FA drops, and can very well skip a sulcus on their way to cortex (Ben-Shachar et al. 2007). Second, error monitoring deficits in speech production have often been proposed as part of the core deficit in stuttering, and this finding has been supported by recent electrophysiological evidence (Arnstein et al. 2011; but see Postma and Kolk 1992 for an alternative view). Future studies will be necessary to determine whether the FAT is related to error monitoring, and whether this relation generalizes to other domains beyond speech.

Within the CST, our data show an increase in MD of AWS compared with controls, in the inferior portion of the left tract. The pattern of this result is in agreement with a recent study that shows a significant reduction in FA values measured in the cerebellar peduncles of people who stutter compared with controls (Figure 4 of Connally et al. 2013). Both studies are compatible with less restricted diffusivity in the CST at the level of the cerebellar peduncles in people who stutter. Moreover, each of these studies extends this information in complementary ways: Our results indicate that the difference is limited to the left tract, while the study by Connally et al. (2013) shows that the differences extend over the inferior, middle and superior cerebellar peduncles (each averaged across the two hemispheres). In our sample of participants, FA values of the CST did not differ significantly between the groups. Previous studies of developmental stuttering that report FA differences in the CST used whole brain voxel-based methods (Cai et al. 2014; Chang et al. 2008; Watkins et al. 2008). Interestingly, the one study that used both tractography and Tract-Based-Spatial-Statistics (TBSS) reported FA differences in the CST only when using TBSS (Connally et al. 2013). Therefore, the discrepancy between our results and the previous reports of stuttering-related FA differences in the CST may be caused by the different methodologies that were employed.

In this study, we report differences in MD that are not accompanied by parallel differences in FA. Although it is common to find MD and FA effects that go in opposite directions, the two metrics are not necessarily correlated (Figure 6 of De Santis et al. 2014). MD and FA provide complementary information about the eigenvalues obtained during tensor fit: While MD measures the average of the three eigenvalues of the tensor, FA quantifies their normalized standard deviation. An MD difference without an

FA difference suggests an overall difference in eigenvalues which is not specific to one direction of diffusivity, and thus does not translate into a difference in anisotropy. Indeed, we show that the increase in MD is derived from an increase in both AD and RD (Figs. 4, 5). Such a pattern of joint increase in AD and RD implies that within these tracts there are fewer constraints to diffusion (reduced tissue density) in a manner not specific to a certain direction.

MD values rely on water diffusion that is sensitive to the microstructure of the underlying brain tissue, yet the interpretation of these values in terms of tissue properties should be attempted cautiously (Jones et al. 2013). In white matter, MD values are affected by many factors including water content, membrane density, myelin and axonal count (Alexander et al. 2007; Burzynska et al. 2010; Schmierer et al. 2007). Any combination of these factors may have conspired to generate the effects reported here, but most would affect FA in an opposite manner. We hypothesize that increased MD values in AWS could stem from a combination of factors: For example, noisy communication (reduced synchrony) between the IFG and SMA could have led to excessive pruning of axons through the FAT, increasing MD and reducing FA, as well as to a more coherent fiber organization within the FAT, which would elevate FA back to its typical range. Elevated membrane permeability has similarly been proposed as a mechanism to explain developmental differences in MD that covary with slowed information transfer, without affecting FA (Scantlebury et al. 2014). Admittedly, such hypotheses are impossible to test directly with DTI alone, and would be more directly testable using imaging methods geared for quantifying more specific tissue properties (e.g., Assaf et al. 2008; Mezer et al. 2013; Stikov et al. 2011).

MD values may be affected by other factors that stem from the methodology, like partial volume averaging across different tissue types and crossing fibers (Vos et al. 2011, 2012). We consider partial volume effects an unlikely explanation for the effects reported here because the anisotropy values in regions that showed a significant group difference were greater than 0.35 (values typical to white matter), and because the FAT is not directly adjacent to the ventricles, as verified by individual inspection of the tracts. Thus, FAT voxels are unlikely to partially sample gray matter or CSF in addition to white matter.

Functionally, our results show that lower MD values are associated with a person's ability to produce more syllables during a fixed time period. This implies that in this sample of AWS, lower MD values predict faster transmission between inferior frontal language regions and the pre-SMA/SMA involved in speech planning and production. This interpretation of the results is in agreement with previous reports in either older adults, younger adults or children, linking lower MD values with enhanced processing speed, and therefore with faster transmission between cortical regions (Bakhtiari et al. 2014; Sasson et al. 2010; Scantlebury et al. 2014). Future studies are expected to shed more light on this idea using methods that tap into more specific tissue properties, combined with direct estimates of transmission speed (Horowitz et al. 2014).

## Limitations

Several limitations of the current study should be acknowledged. First, the sample size is limited ($N = 15$ and 19 for AWS and controls, respectively), which reduces the statistical power of our analyses. However, even with this limited power, we were able to detect significant differences in diffusion properties between AWS and controls, as well as within group correlations with behavior. This limitation is still relevant to null effects reported here, particularly the absence of significant group differences in FA. A recent analysis has shown that MD requires a relatively smaller sample size compared with FA, for the detection of equivalent effect sizes (De Santis et al. 2014). It is therefore possible that future studies with larger samples will detect FA differences that have not been detected here. Second, our sample spans a relatively large age range (19–52 years old participants in both groups). While the groups were well-matched in mean-age and age range (see Table 1), this age range still raises the concern that age could somehow drive the effects we find, especially given the known variation in white matter properties during adulthood (Lebel et al. 2012b). To address this concern, we conducted ANCOVA analyses with Age as a covariate to examine the contribution of age to the group differences that were found, and we calculated partial correlations to control for the effect of Age on the brain-behavior correlations that showed a significant effect. None of these analyses indicated a significant contribution of Age to the reported effects. Third, in this study we used a scan protocol with limited angular resolution (19 diffusion directions). We chose this number of directions to ensure a short duration scan (5:50 min) that will reduce the chance of within scan head motion, and we improved the signal-to-noise ratio by repeating the acquisition twice. While simulation studies recommend the use of at least 30 diffusion gradient-encoding directions for the purpose of tractography (Jones 2004), a study of human subjects demonstrated that similarly robust measurements are achieved using 6 and 30 directions in many white matter tracts delineated using deterministic tractography (Lebel et al. 2012a). The authors of the latter study conclude that using repeated scans (as used here) along with at least six directions (we use 19) should be considered appropriate for the purposes of deterministic tractography.

## Conclusions

Our study shows differences in diffusion measures of the bilateral frontal aslant tract and the left CST in persistent developmental stuttering. Further, the data show an association between diffusion measures of the left frontal aslant tract and behavioral measures of speech fluency in adults who stutter. This association is anatomically selective in that it does not hold in the other tracts targeted here, or in controls. By demonstrating the involvement of the bilateral frontal aslant tracts in persistent developmental stuttering, our findings strengthen the view that this tract plays a role in the production of fluent speech and should be considered in future studies of language and its disorders.

**Acknowledgments** This work was supported by the Israel Science Foundation (ISF grant 513/11 awarded to M.B.-S and O.A) and by the Israeli Center of Research Excellence in Cognition (I-CORE Program 51/11 of the Planning and Budgeting Committee). O.C. was supported by the Israeli Ministry of Immigrant Absorption. We thank the Israeli Stuttering Association (AMBI) for their help with participant recruitment. We thank the team at the Wohl institute for advanced imaging in Tel Aviv Sourasky Medical Center, for their assistance with protocol setup and MRI scanning. We thank Jason Yeatman for his assistance with adjustments in the AFQ code. Finally, we are grateful to Prof. Yaniv Assaf and to Maya Yablonski for their helpful comments.

**Conflict of interest** The authors declare that there are no conflicts of interest.

## References

Akers D (2006) CINCH: a cooperatively designed marking interface for 3D pathway selection. Paper presented at the User Interface Software and Technology meeting, Montreux

Alexander AL, Lee JE, Lazar M, Field AS (2007) Diffusion tensor imaging of the brain. Neurotherapeutics 4:316–329

Alm PA (2004) Stuttering and the basal ganglia circuits: a critical review of possible relations. J Commun Disord 37:325–369

Ambrose NG, Yairi E (1999) Normative disfluency data for early childhood stuttering. J Speech Lang Hear Res 42:895–909

Amir O, Levine-Yundof R (2013) Listeners' attitude toward people with dysphonia. J Voice 27:524.e1–524.e10

Arnstein D, Lakey B, Compton RJ, Kleinow J (2011) Preverbal error-monitoring in stutterers and fluent speakers. Brain Lang 116:105–115

Assaf Y, Blumenfeld-Katzir T, Yovel Y, Basser PJ (2008) AxCaliber: a method for measuring axon diameter distribution from diffusion MRI. Magn Reson Med 59:1347–1354

Bakhtiari R, Boliek C, Cummine J (2014) Investigating the contribution of ventral-lexical and dorsal-sublexical pathways during reading in bilinguals. Front Hum Neurosci 8:507

Basser PJ, Pierpaoli S (1996) Microstructural and physiological features of tissues elucidated by quantitative diffusion tensor MRI. J Magn Reson 111:209–219

Basser PJ, Pajevic S, Pierpaoli S, Duda J, Aldroubi A (2000) In vivo fiber tractography using DT-MRI data. Magn Reson Med 44:625–632

Beal DS, Gracco VL, Lafaille SJ, De Nil LF (2007) Voxel-based morphometry of auditory and speech-related cortex in stutterers. NeuroReport 18:1257–1260

Beal DS, Gracco VL, Brettschneider J, Kroll RM, De Nil LF (2013) A voxel-based morphometry (VBM) analysis of regional grey and white matter volume abnormalities within the speech production network of children who stutter. Cortex 49:2151–2216

Benjamini Y, Hochberg Y (1995) Controlling the false discovery rate: a practical and powerful approach to multiple testing. J R Stat Soc Ser B (Methodol) 57:289–300

Ben-Shachar M, Dougherty RF, Wandell BA (2007) White matter pathways in reading. Curr Opin Neurobiol 17:258–270

Biermann-Ruben K, Salmelin R, Schnitzler A (2005) Right rolandic activation during speech perception in stutterers: a MEG study. Neuroimage 25:793–801

Bloodstein O, Ratner NB (2008) A handbook on stuttering, 6th edn. Delmar, Stamford

Braun A et al (1997) Altered patterns of cerebral activity during speech and language production in developmental stuttering. An H2(15)O positron emission tomography study. Brain 120:761–784

Brown S, Ingham RJ, Ingham JC, Laird AR, Fox PT (2005) Stuttered and fluent speech production: an ALE meta-analysis of functional neuroimaging studies. Hum Brain Mapp 25:105–117

Burzynska AZ, Preuschhof C, Bäckman L, Nyberg L, Li S-C, Lindenberger U, Heekeren HR (2010) Age-related differences in white matter microstructure: region-specific patterns of diffusivity. Neuroimage 49:2104–2112

Cai S, Tourville JA, Beal DS, Perkell JS, Guenther FH, Ghosh SS (2014) Diffusion imaging of cerebral white matter in persons who stutter: evidence for network-level anomalies. Front Hum Neurosci 8:54

Catani M et al (2012) Short frontal lobe connections of the human brain. Cortex 48:273–291

Catani M et al (2013) A novel frontal pathway underlies verbal fluency in primary progressive aphasia. Brain 136:2619–2628

Chang S-E, Erickson KI, Ambrose NG, Hasegawa-Johnson MA, Ludlow CL (2008) Brain anatomy differences in childhood stuttering. Neuroimage 39:1333–1344

Chang S-E, Kenney MK, Loucks TMJ, Ludlow CL (2009) Brain activation abnormalities during speech and non-speech in stuttering speakers. Neuroimage 46:201–212

Chang S-E, Synnestvedt A, Ostuni J, Ludlow CL (2010) Similarities in speech and white matter characteristics in idiopathic developmental stuttering and adult-onset stuttering. J Neurolinguist 23:455–469

Chang S-E, Horwitz B, Ostuni J, Reynolds R, Ludlow CL (2011) Evidence of left inferior frontal premotor structural and functional connectivity deficits in adults who stutter. Cereb Cortex 21:2507–2518

Cogan GB, Thesen T, Carlson C, Doyle W, Devinsky O, Pesaran B (2014) Sensory-motor transformations for speech occur bilaterally. Nature 507:94–98

Connally EL, Ward D, Howell P, Watkins KE (2013) Disrupted white matter in language and motor tracts in developmental stuttering. Brain Lang 6:256–266

Corder GW, Foreman DI (2009) Nonparametric statistics for non-statisticians: a step-by-step approach. Wiley, Hoboken

Cykowski MD, Fox PT, Ingham RJ, Ingham JC, Robin DA (2010) A study of the reproducibility and etiology of diffusion anisotropy differences in developmental stuttering: a potential role for impaired myelination. Neuroimage 52:1495–1504

De Santis S, Drakesmith M, Bells S, Assaf Y, Jones DK (2014) Why diffusion tensor MRI does well only some of the time: variance and covariance of white matter tissue microstructure attributes in the living human brain. Neuroimage 89:35–44

Dick AS, Bernal B, Tremblay P (2013) The language connectome new pathways, new concepts. Neuroscientist 20(5):453–467

Dosenbach NU et al (2006) A core system for the implementation of task sets. Neuron 50:799–812

Dougherty RF, Ben-Shachar M, Deutsch GK, Hernandez A, Fox GR, Wandell BA (2007) Temporal-callosal pathway diffusivity predicts phonological skills in children. PNAS 104:8556–8561

Eckert MA, Menon V, Walczak A, Ahlstrom J, Denslow S, Horwitz A, Dubno JR (2009) At the heart of the ventral attention system: the right anterior insula. Hum Brain Mapp 30:2530–2541

Finkelstein M, Amir O (2013) Speaking rate among professional radio newscasters: Hebrew speakers. Stud Media Commun 1:131–139

Fonov V, Evans AC, Botteron K, Almli CR, McKinstry RC, Collins DL (2011) Unbiased average age-appropriate atlases for pediatric studies. Neuroimage 54:313–327

Ford A, McGregor KM, Case K, Crosson B, White KD (2010) Structural connectivity of Broca's area and medial frontal cortex. Neuroimage 52:1230–1237

Foundas AL, Bollich AM, Feldman J, Corey DM, Hurley M, Lemen LC, Heilman KM (2004) Aberrant auditory processing and atypical planum temporale in developmental stuttering. Neurology 63:1640–1646

Fox PT, Ingham RJ, Ingham JC, Zamarripa F, Xiong JH, Lancaster JL (2000) Brain correlates of stuttering and syllable production. A PET performance-correlation analysis. Brain 123:1985–2004

Friston KJ, Ashburner J (2004) Generative and recognition models for neuroanatomy. Neuroimage 23:21–24

Hickok G, Poeppel D (2007) The cortical organization of speech processing. Nat Rev Neurosci 8:393–402

Horowitz A, Barazany D, Tavor I, Bernstein M, Yovel G, Assaf Y (2014) In vivo correlation between axon diameter and conduction velocity in the human brain. Brain Struct Funct, 1–12

Jäncke L, Hänggi J, Steinmetz H (2004) Morphological brain differences between adult stutterers and non-stutterers. BMC Neurol 4:23

Jones DK (2004) The effect of gradient sampling schemes on measures derived from diffusion tensor MRI: a Monte Carlo study. Magn Reson Med 51:807–815

Jones DK, Knösche TR, Turner R (2013) White matter integrity, fiber count, and other fallacies: the do's and don'ts of diffusion MRI. Neuroimage 73:239–254

Kell CA, Neumann K, Kriegstein KV, Posenenske C, Gudenberg AWV, Euler H, Giraud A-L (2009) How the brain repairs stuttering. Brain 132:2747–2760

Kushner HI (2012) Retraining left-handers and the aetiology of stuttering: the rise and fall of an intriguing theory. Laterality: asymmetries of body. Brain Cogn 17:673–693

Lawes INC, Barrick TR, Murugam V, Spierings N, Evans DR, Song M, Clark CA (2008) Atlas-based segmentation of white matter tracts of the human brain using diffusion tensor tractography and comparison with classical dissection. Neuroimage 39:62–79

Lebel C, Benner T, Beaulieu C (2012a) Six is enough? Comparison of diffusion parameters measured using six or more diffusion-encoding gradient directions with deterministic tractography. Magn Reson Med 68:474–483

Lebel C, Gee M, Camicioli R, Wieler M, Martin W, Beaulieu C (2012b) Diffusion tensor imaging of white matter tract evolution over the lifespan. Neuroimage 60:340–352

Leemans A, Jones DK (2009) The B-matrix must be rotated when correcting for subject motion in DTI data. Magn Reson Med 61:1336–1349

Lu C et al (2010a) The neural substrates for atypical planning and execution of word production in stuttering. Exp Neurol 221(1):146–156

Lu C et al (2010b) Altered effective connectivity and anomalous anatomy in the basal ganglia-thalamocortical circuit of stuttering speakers. Cortex 46:49–67

MacDonald CM, Mallard A (1979) Word-by-word analysis of observer agreement utilizing audio and audiovisual techniques. J Fluency Disord 4:23–28

Mezer A et al (2013) Quantifying the local tissue volume and composition in individual brains with MRI. Nat Med 19:1667–1672

Moore WH Jr (1984) Central nervous system characteristics of stutterers. In: Curlee R, Perkins WH (eds) Nature and treatment of stuttering: new directions. College-Hill Press, San Diego

Mori S, Crain BJ, Chacko V, Van Zijl P (1999) Three-dimensional tracking of axonal projections in the brain by magnetic resonance imaging. Ann Neurol 45:265–269

Nichols TE, Holmes AP (2002) Nonparametric permutation tests for functional neuroimaging: a primer with examples. Hum Brain Mapp 15:1–25

Oldfield RC (1971) The assessment and analysis of handedness: the Edingburgh inventory. Neuropsychologia 9:97–113

Perkins WH, Kent RD, Curlee RF (1991) A theory of neuropsycholinguistic function in stuttering. J Speech Hear Res 34:734–752

Postma A, Kolk H (1992) Error monitoring in people who stutter: evidence against auditory feedback defect theories. J Speech Lang Hear Res 35:1024–1032

Postma A, Kolk H (1993) The covert repair hypothesis: prearticulatory repair process in normal and sttuttered disfluencies. J Speech Hear Res 36:49–59

Preibisch C, Neumann K, Raab P, Euler H, von Gudenberg A, Lanfermann H, Giraud A (2003) Evidence for compensation for stuttering by the right frontal operculum. Neuroimage 20:1356–1364

Rhode GK, Barnett AS, Basser PJ, Marenco S, Pierpaoli S (2004) Comprehensive approach for correction of motion and disortion in diffusion-weighted MRI. Magn Reson Med 51:103–114

Riley G (1994) Stuttering severity instrument for children and adults, 3rd edn. Pro-Ed, Austin

Rochman D, Amir O (2013) Examining in-session expressions of emotions with speech/vocal acoustic measures: an introductory guide. Psychother Res 23:381–393

Sasson E, Doniger G, Pasternak O, Assaf Y (2010) Structural correlates of memory performance with diffusion tensor imaging. Neuroimage 50:1231–1242

Sasson E, Doniger GM, Pasternak O, Tarrasch R, Assaf Y (2012) Structural correlates of cognitive domains in normal aging with diffusion tensor imaging. Brain Struct Funct 217:503–515

Sasson E, Doniger GM, Pasternak O, Tarrasch R, Assaf Y (2013) White matter correlates of cognitive domains in normal aging with diffusion tensor imaging. Front Neurosci 7:32

Scantlebury N et al (2014) Relations between white matter maturation and reaction time in childhood. J Int Neuropsychol Soc 20:99–112

Schmierer K et al (2007) Diffusion tensor imaging of post mortem multiple sclerosis brain. Neuroimage 35:467–477

Sheskin DJ (2003) Handbook of parametric and nonparametric statistical procedures, 3rd edn. CRC Press, Boca Raton

Smith A (1999) Stuttering: a unified approach to a multifactorial, dynamic disorder. In: Ratner NB, Healey EC (eds) Stuttering reaserch and practice: bridging the gap. Lawrence Erlbaum Associates Inc, NJ

Smith A, Goffman L, Sasisekaran J, Weber-Fox C (2012) Language and motor abilities of preschool children who stutter: evidence from behavioral and kinematic indices of nonword repetition performance. J Fluency Disord 37:344–358

Sommer M, Koch MA, Paulus W, Weiller C, Büchel C (2002) Disconnection of speech-relevant brain areas in persistent developmental stuttering. Lancet 360:380–383

Stikov N, Perry LM, Mezer A, Rykhlevskaia E, Wandell BA, Pauly JM, Dougherty RF (2011) Bound pool fractions complement diffusion measures to describe white matter micro and macrostructure. Neuroimage 54:1112–1121

Thiebaut de Schotten M et al (2011) Atlasing location, asymmetry and inter-subject variability of white matter tracts in the human brain with MR diffusion tractography. Neuroimage 54:49–59

Travis L (1931) Speech pathology. Appelton-Century, New York

Tzourio-Mazoyer N et al (2002) Automated anatomical labeling of activations in SPM using a macroscopic anatomical parcellation of the MNI MRI single-subject brain. Neuroimage 15:273–289

Vaden KI, Kuchinsky SE, Cute SL, Ahlstrom JB, Dubno JR, Eckert MA (2013) The cingulo-opercular network provides word-recognition benefit. J Neurosci 33:18979–18986

Vassal F, Boutet C, Lemaire J-J, Nuti C (2014) New insights into the functional significance of the frontal aslant tract-An anatomo-functional study using intraoperative electrical stimulations combined with diffusion tensor imaging-based fiber tracking. Br J Neurosurg 28:685–687

Vos SB, Jones DK, Viergever MA, Leemans A (2011) Partial volume effect as a hidden covariate in DTI analyses. Neuroimage 55:1566–1576

Vos SB, Jones DK, Jeurissen B, Viergever MA, Leemans A (2012) The influence of complex white matter architecture on the mean diffusivity in diffusion tensor MRI of the human brain. Neuroimage 59:2208–2216

Wakana S et al (2007) Reproducibility of quantitative tractography methods applied to cerebral white matter. Neuroimage 36:630–644

Watkins KE, Smith SM, Davis S, Howell P (2008) Structural and functional abnormalities of the motor system in developmental stuttering. Brain 131:50–59

Williams DE, Wark M, Minifie FD (1963) Ratings of stuttering by audio, visual, and audiovisual cues. J Speech Lang Hear Res 6:91

Xuan Y et al (2012) Resting-state brain activity in adult males who stutter. PLoS ONE 7:e30570

Yairi E, Ambrose NG (2005) Early childhood stuttering for clinicians by clinicians. PRO-ED, Austin

Yeatman JD, Dougherty RF, Rykhlevskaia E, Sherbondy AJ, Deutsch GK, Wandell BA, Ben-Shachar M (2011) Anatomical properties of the arcuate fasciculus predict phonological and reading skills in children. J Cogn Neurosci 23:3304–3317

Yeatman JD, Dougherty RF, Myall NJ, Wandell BA, Feldman HM (2012) Tract profiles of white matter properties: automating fiber-tract quantification. PLoS ONE 7:e49790